Research Article

Salvianolic Acid B Suppresses Non-Small-Cell Lung Cancer Metastasis through PKM2-Independent Metabolic Reprogramming

Hong Zhang, Jianming Tang, Yu Cao, and Tianhu Wang (iD)

Department of Thoracic Surgery, The Third Affiliated Hospital of Chongqing Medical University, Chongqing 401120, China

Correspondence should be addressed to Tianhu Wang; wtianhu@hospital.cqmu.edu.cn

Objective. Salvianolic acid B (Sal B) has been demonstrated to be a potential chemoprevention agent for several cancers. Herein, we investigated the pharmacological function of Sal B on non-small-cell lung cancer (NSCLC) metastasis. *Methods.* Two NSCLC cell lines (NCI-H2030 and NCI-H1650) were disposed of by $200 \mu M$ Sal B or $10 \mu M$ PKM2 agonist TEPP-46. Wound healing and transwell experiments were implemented for analyzing migratory and invasive capacities. Epithelial-to-mesenchymal transition (EMT) markers β-catenin and E-cadherin were measured via western blotting. Cellular bioenergetics were evaluated with glucose uptake, lactate production, enolase activity, cellular ATP levels, as well as seahorse-based oxygen consumption rate (OCR), extracellular acidification rate (ECAR) analysis. Metabolic reprogramming markers PKM2, LDHA, and GLUT1 were detected via western blotting and immunofluorescence. *Results.* The results showed that Sal B disposal weakened the migration and invasion of NCI-H2030 and NCI-H1650 cells and inactivated the EMT process according to downregulation of β-catenin and upregulation of E-cadherin. Sal B-treated NSCLC cells displayed decreased glucose uptake, lactate production, enolase activity, cellular ATP levels, OCR, and ECAR, indicating a reduction in metabolic reprogramming. Additionally, Sal B downregulated the expression of PKM2, LDHA, and GLUT1. TEPP-46 may reverse the inhibitory effect of Sal B on metastasis as well as metabolic reprogramming. *Conclusion.* Our findings provide evidence that Sal B enables to weaken NSCLC metastasis through PKM2-independent metabolic reprogramming, which sheds light on the promising therapeutic usage of Sal B in treating NSCLC.

1. Introduction

Non-small-cell lung cancer (NSCLC) is the most frequent and deadly type of primary lung malignancy, occupying 85% of all cases [1, 2]. It is histologically classified as adenocarcinoma, squamous cell carcinoma as well as large-cell carcinoma [3, 4]. Distant metastasis represents the dominating cause of mortality in NSCLC [5]. For resectable NSCLC tumors, primary treatment includes surgery with or without neoadjuvant therapy [6]. The mainstay of treatment for nonresectable tumors is radiotherapy and systemic treatments that are also offered for palliative treatment [7]. Systemic treatment contains conventional chemotherapy that is usually linked to remarkable side effects, targeted molecular treatment (such as tyrosine kinase inhibitors), as well as immunotherapies (such as immune-checkpoint

inhibitors) [8]. Nevertheless, clinical drug resistance or nonresponse remains a challenge, which greatly hinders treatment success [9].

Many advances have been made in the comprehending of the pathophysiology of NSCLC metastasis. NSCLC is characterized by increased glucose and lactate utilization, and widespread heterogeneity in metabolic signaling [10]. Metabolic reprogramming represents a hallmark of cancer, and targeting metabolism has become a promising therapeutic strategy against NSCLC [11]. Pyruvate kinase may physiologically irreversibly catalyze phosphoenolpyruvate to pyruvate as a kinase in the final step of glycolysis [12]. Only tumor cells express the embryonic M2 isoform of pyruvate kinase (PKM2). As a crucial rate-limiting enzyme in glycolysis, PKM2 exerts an important function in the metabolic reprogramming of tumor cells [13]. The upregulation has

been demonstrated in NSCLC, and secreted PKM2 facilitates NSCLC metastasis via activation of integrin $\beta 1$/FAK signaling [14]. Thus, targeting PKM2 represents a potential therapeutic regimen of NSCLC.

Chemoprevention is considered a reasonable and attractive strategy to prevent or delay the development of NSCLC [15]. Chinese herbal medicine Salviae miltiorrhizae has been broadly applied in traditional Chinese medicine practice in treating cardiovascular and cerebrovascular diseases with minimal side effects [16]. Salvianolic acid B (Sal-B), extracted from the root of Salviae miltiorrhizae, is a major bioactive hydrophilic ingredient [17]. Several studies have demonstrated the anticancer pharmacological properties of Sal-B. For instance, Sal-B restrains glioma cells that are sensitive to radiotherapy through Fis-1-independent mitochondrial dysfunction [18]. Sal-B suppresses the growth of head and neck squamous cell carcinoma through cyclooxygenase-2 and apoptotic signaling [19]. Nevertheless, the pharmacological properties of Sal-B on anti-NSCLC remain indistinct. Here, we aimed to investigate the therapeutic effect of Sal-B on NSCLC metastasis. Our findings demonstrated that Sal B may weaken NSCLC metastasis with PKM2-independent metabolic reprogramming.

2. Materials and Methods

2.1. Cell Culture and Reagents. To investigate the therapeutic effect of Sal-B on NSCLC metastasis, two NSCLC cell lines (NCI-H2030 and NCI-H1650; ATCC, USA) were selected. All cells were grown in DMEM (Hyclone, USA) plus 10% fetal bovine serum (FBS; Hyclone) at 37°C in a humidified environment of 5% CO_2. Sal B (purity ≥98%; Hongqiao Pharmaceutical Technology Research Institute Co., Ltd., Nanjing, China) was dissolved in absolute ethanol to 50 mM and stored at −80°C. Moreover, TEPP-46 was acquired from MedChemExpress Company (USA). NSCLC cell lines were treated with 10 μM TEPP-46 for selectively activating pyruvate kinase M2 (PKM2).

2.2. Cell Counting Kit-8 (CCK-8). NCI-H2030 and NCI-H1650 cells were inoculated into a 96-well plate lasting 24 hours. Thereafter, they were exposed to 0, 100, 200, 300, 400, 500, or 600 μM Sal B lasting 24 or 48 hours. Following removing the cell culture medium with Sal B, the cells were treated with 100 μL of cell culture medium plus 10% CCK-8 (Dojindo, Japan) lasting 4 hours. Optical densities were finally measured.

2.3. Wound Healing Assay. NCI-H2030 and NCI-H1650 cells were inoculated onto a 24-well plate. When subconfluence was reached, wound healing was made to the cell monolayers utilizing 200 μL pipette tips. At 48 hours, wound healing was captured under light microscopy (×200; Leica, Germany), and the relative migration level was measured.

2.4. Transwell Assay. The Transwell assay with Matrigel (Sigma-Aldrich, USA) was implemented utilizing a 24-well plate with Transwell chambers (8 μm pore; Sigma-Aldrich).

The bottom chambers were added to with DMEM containing 20% FBS. 5×10^4 NCI-H2030 and NCI-H1650 cells were inoculated into the upper chambers with serum-free medium. Migratory cells were fixed by 4% formaldehyde, stained with 1% crystal violet, followed by counting under light microscopy (×200; Leica, Germany).

2.5. Western Blotting. Protein extraction from NCI-H2030 and NCI-H1650 cells was implemented via the RIPA solution (P0013C; Beyotime, China). Protein concentrations were tested utilizing BCA assay kits (P0011; Beyotime). The extracted proteins were denatured in boiling water for 15-minutes. Thereafter, electrophoresis was carried out utilizing 10% SDS-PAGE gel for separation of protein molecules. Following protein transference onto PVDF membranes, the proteins were blocked in 5% nonfat milk at room temperature for 2 hours. Afterwards, incubation with primary antibody of β-catenin (1/1000; ab265591; Abcam, USA), E-cadherin (1/2000; ab231303), GAPDH (1/2500; ab9485), PKM2 (1/1000; #4053; Cell Signaling Technology, USA), phosphorylated PKM2 (p-PKM2; 1/1000; #3827; Cell Signaling Technology), lactate dehydrogenase A (LDHA; 1/1000; #3582; Cell Signaling Technology), and glucose transporter 1 (GLUT1; 1/1000; #73015; Cell Signaling Technology) was implemented at 4°C lasting 18 hours, followed by incubation with IgG-HRP goat anti-rabbit (1/3000; #7074; Cell Signaling Technology) for 2 hours. Signals were developed with ECL (Sigma-Aldrich) and normalized.

2.6. Glucose Uptake and Lactate Production. Glucose uptake was determined utilizing the glucose uptake assay kit (ab136955; Abcam) in accordance with the manufacturer's specification. Cell lysate was harvested as well as measured for lactate level utilizing the lactate assay kit (ab65330; Abcam) in accordance with the manufacturer's specification. The optical density value of cell lysate was measured after 24 hours. Lactate production was tested according to standard curves, followed by normalization to the cell lysate concentration.

2.7. Measurement of Enolase Activity. Enolase activity was measured with an enolase activity assay kit (ab241024; Abcam). In brief, cell lysate was mixed with the reaction buffer. After being incubated for 10 minutes at 25°C, the optical density value was quantified at 570 nm. Thereafter, each subsequent assay was carried out for 2 minutes until the optical density value of the most active specimens exceeded the highest standard. Enolase activity was finally calculated.

2.8. Enhanced ATP Assay. An enhanced ATP assay was carried out utilizing an enhanced ATP assay kit (S0027; Beyotime). The supernatant was added to 100 μl of ATP detection solution. Thereafter, the RLU values were recorded through a Promega Glomax 20/20 luminometer. A standard curve was drawn according to the RLU values of ATP at concentrations of 0, 0.01, 0.05, 0.1, 0.5, 1, 5, and 10 nmol/L.

The protein concentrations were utilized for standardizing the results and are shown as ATP/protein (nmol/mg).

2.9. Seahorse Analysis. Oxygen consumption rate (OCR) and extracellular acidification rate (ECAR) were detected utilizing XF24 extracellular analyzer (Seahorse Bioscience, USA). The 24-well cell culture microplate coated with Corning® Cell-Tak™ Cell as well as tissue adhesive was used for allowing adhesion of suspended cells. Thereafter, sequential compounds containing $1 \mu M$ oligomycin, $0.5 \mu M$ carbonyl-cyanide p-trifluoromethoxy phenylhydrazone (FCCP), and $0.5 \mu M$ antimycin A (antiA)/rotenone (Rot), were added to the microplate for testing mitochondrial respiration. Furthermore, sequential compounds containing 10 mM glucose, $1 \mu M$ oligomycin, and 50 mM 2-deoxyglucose (2-DG), were added for testing glycolytic activity.

2.10. Immunofluorescence. 5×10^4 NCI-H2030 and NCI-H1650 cells were inoculated into chamber slides. They were fixed with 4% paraformaldehyde (P0099; Beyotime) for 15 minutes, as well as permeabilized with 0.1% Triton X-100 (P0096; Beyotime) for 15 minutes. After blocking with 10% goat serum at room temperature, incubation with primary antibodies targeting PKM2 (1/100; #4053; Cell Signaling Technology) and GLUT1 (1/100; #73015; Cell Signaling Technology) was implemented at 4°C, as well as ALexa Fluor 488 conjugated secondary antibody (1/500; #4412; Cell Signaling Technology) and Hoechst 33342 labeling (1/500; #4082; Cell Signaling Technology). The results were imaged under confocal microscopy (×200; Leica).

2.11. Statistical Analysis. Statistical analysis was implemented via GraphPad Prism 8 software (San Diego, USA). The statistical comparison was carried out utilizing Student's *t*-test, one-way analysis of variance (ANOVA) or two-way ANOVA. The data are displayed as the mean ± standard deviation from at least three independent experiments. *P* values <0.05 were considered statistical significance.

3. Results

3.1. Sal B Suppresses Migration and Invasion of NSCLC Cells. For investigation of the therapeutic function of Sal B, two NSCLC cells (NCI-H2030 and NCI-H1650) were exposed to distinct concentrations of Sal B for 24 or 48 hours. As shown in CCK-8, at 24 hours of exposure, when the concentration of Sal B reached $400 \mu M$, the cell viability of NCI-H2030 and NCI-H1650 cells displayed a significant reduction compared with controls (Figures 1(a) and 1(b)). At 48 hours of exposure, cell viability was remarkably decreased until the concentration reached $300 \mu M$ which was higher than controls. This demonstrated that Sal B exposure enabled to weaken the proliferative capacity of NSCLC cells. We further evaluated the therapeutic function of $200 \mu M$ Sal B on NSCLC metastasis. The data from the wound healing assay showed that the migration capacity of NCI-H2030 and NCI-H1650 cells was remarkably weakened by $200 \mu M$ Sal B

(Figures 1(c)–1(e)). Additionally, $200 \mu M$ Sal B significantly reduced the invasion capacity of NCI-H2030 and NCI-H1650 cells (Figures 1(f)–1(h)). Hence, Sal B treatment enabled to suppress NSCLC metastasis.

3.2. Sal B Weakens Epithelial-Mesenchymal Transition (EMT) Process in NSCLC Cells. EMT, a reversible developmental genetic program for transdifferentiating polarized epithelial cells to mesenchymal cells, enables to trigger metastasis during the progression of NSCLC [20]. Further analysis showed that $200 \mu M$ Sal B markedly reduced β-catenin expression as well as elevated E-cadherin expression in NCI-H2030 as well as NCI-H1650 cell lines (Figures 2(a)–2(f)), indicating that Sal B enabled to inactivate EMT process of NSCLC cells.

3.3. Sal B Weakens Metabolic Reprogramming of NSCLC Cells. Metabolic reprogramming has been widely recognized as a cancer hallmark [13]. Further analysis was implemented for evaluating the therapeutic function of Sal B on the metabolic reprogramming of NSCLC cells. Compared with controls, $200 \mu M$ Sal B-treated NCI-H2030 and NCI-H1650 cells presented remarkably reduced glucose uptake, lactate production, enolase activity as well as cellular ATP production (Figures 3(a)–3(d)). To evaluate mitochondrial respiration, we measured OCR after adding sequential compounds containing $1 \mu M$ oligomycin, $0.5 \mu M$ FCCP, and $0.5 \mu M$ Rot/antiA. As a result, $200 \mu M$ Sal B prominently decreased OCR both in NCI-H2030 and NCI-H1650 cells than controls (Figures 3(e)–3(h)). We also evaluated glycolytic activity through measuring ECAR following sequential compounds containing 10 mM glucose, $1 \mu M$ oligomycin, and 50 mM 2-DG. The data showed that $200 \mu M$ Sal B-treated NCI-H2030 and NCI-H1650 cells displayed significantly decreased ECAR than controls (Figures 3(i)–3(l)). Altogether, Sal B enabled to weaken the metabolic reprogramming of NSCLC cells.

3.4. Sal B Inhibits PKM2-Mediated Metabolic Reprogramming of NSCLC Cells. PKM2 is a central regulator of aerobic glycolysis of cancer cells, which accelerates lactate production as well as metabolic reprogramming [21]. Our western blotting showed that $200 \mu M$ Sal B-treated NCI-H2030 and NCI-H1650 cells displayed remarkably reduced expression of PKM2 and p-PKM2 in comparison to controls (Figures 4(a)–4(f)). Immunohistochemistry also demonstrated that Sal B was able to decrease PKM2 expression in NCI-H2030 and NCI-H1650 cells (Figures 4(g) and 4(h)). Thus, Sal B inhibited PKM2-mediated metabolic reprogramming of NSCLC cells.

3.5. Sal B Restrains Metabolic Reprogramming-Relevant Genes LDHA and GLUT1 in NSCLC Cells. We also assessed the effects of Sal B on the metabolic reprogramming-relevant genes LDHA and GLUT1 in NSCLC cells. As a result, in comparison to controls, $200 \mu M$ Sal B remarkably reduced the expression of LDHA and GLUT1 both in NCI-H2030
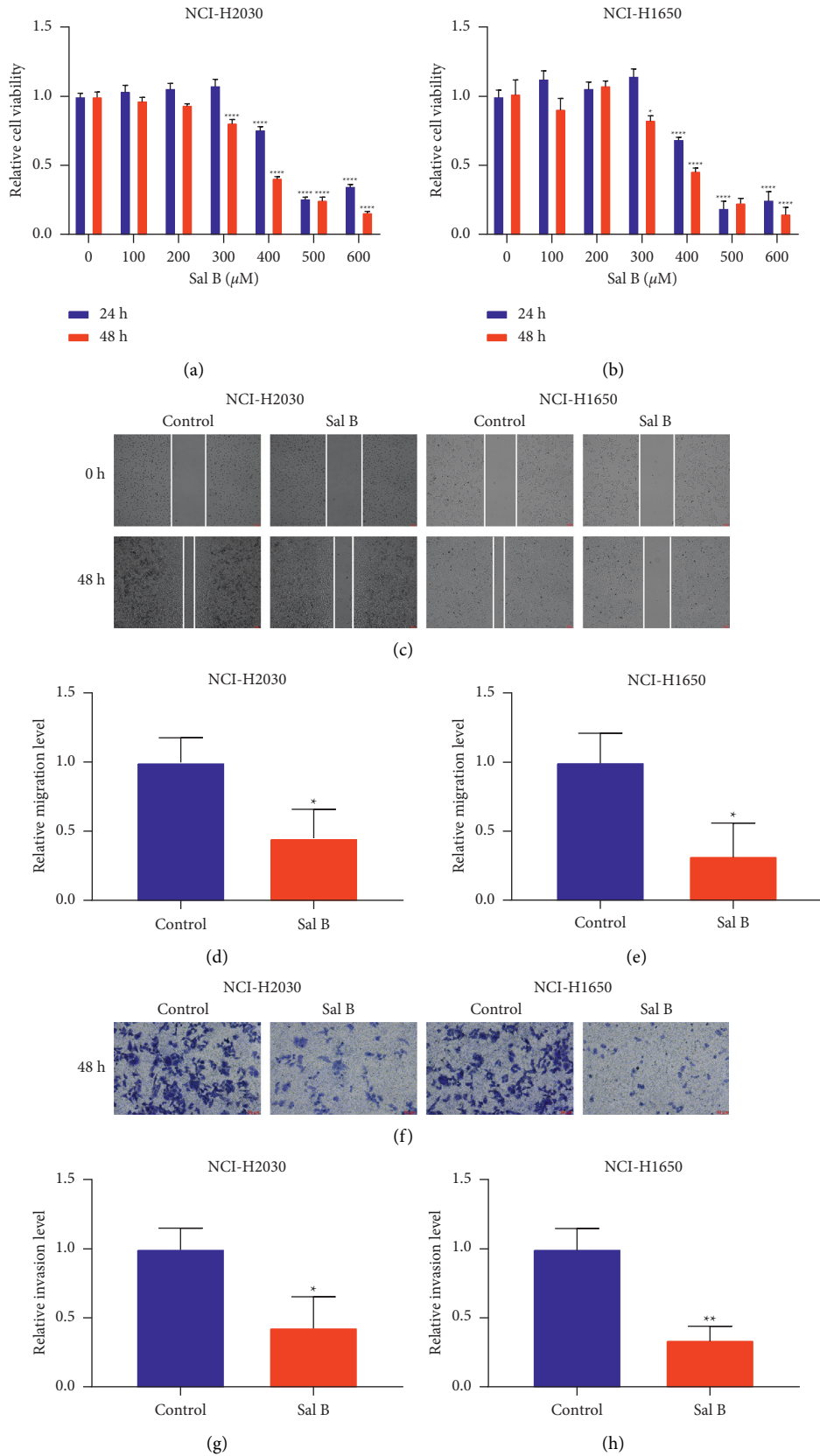
FIGURE 1: Sal B suppresses migration and invasion of NSCLC cells. (a, b) Cell viability of NCI-H2030 and NCI-H1650 cells that were exposed to a series of concentrations of Sal B lasting 24 or 48 hours through CCK-8. (c–e) Wound healing for assessing migration of 200 μM Sal B-treated NCI-H2030 and NCI-H1650 cells. Bar = 50 μM. (f–h) Evaluation of invasion of 200 μM Sal B-treated NCI-H2030 and NCI-H1650 cells through transwell. Bar = 50 μM. $^*P < 0.05$; $^{**}P < 0.01$; $^{****}P < 0.0001$.
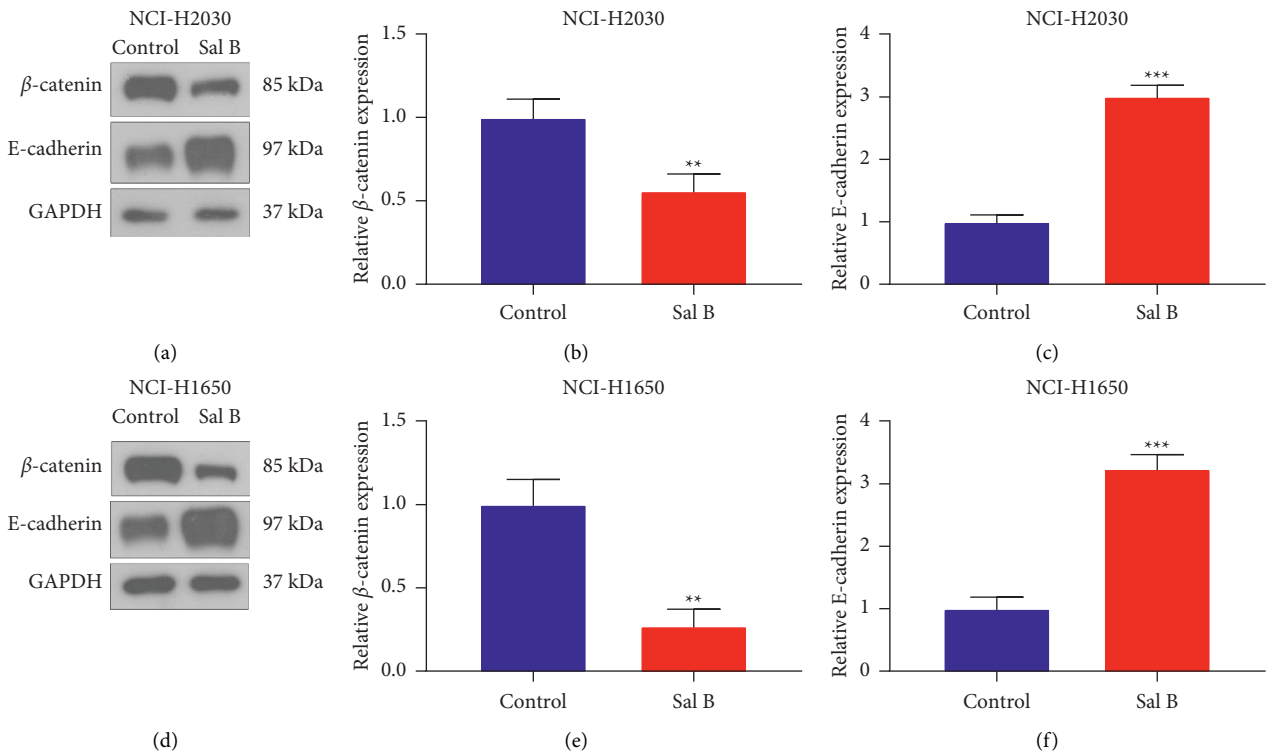
(a)

(b)

(c)

(d)

(e)

(f)

FIGURE 2: Sal B weakens EMT process of NSCLC cells. (a–c) Western blotting of the expression of β-catenin and E-cadherin in 200 μM Sal B-treated NCI-H2030 cells. (d–f) Western blotting of the expression of β-catenin and E-cadherin in 200 μM Sal B-treated NCI-H1650 cells. $^{**}P < 0.01$; $^{****}P < 0.0001$.

(a)

(b)

(c)

(d)

(e)

(f)

FIGURE 3: Continued.

(g)

(h)

(i)

(j)

(k)

(l)
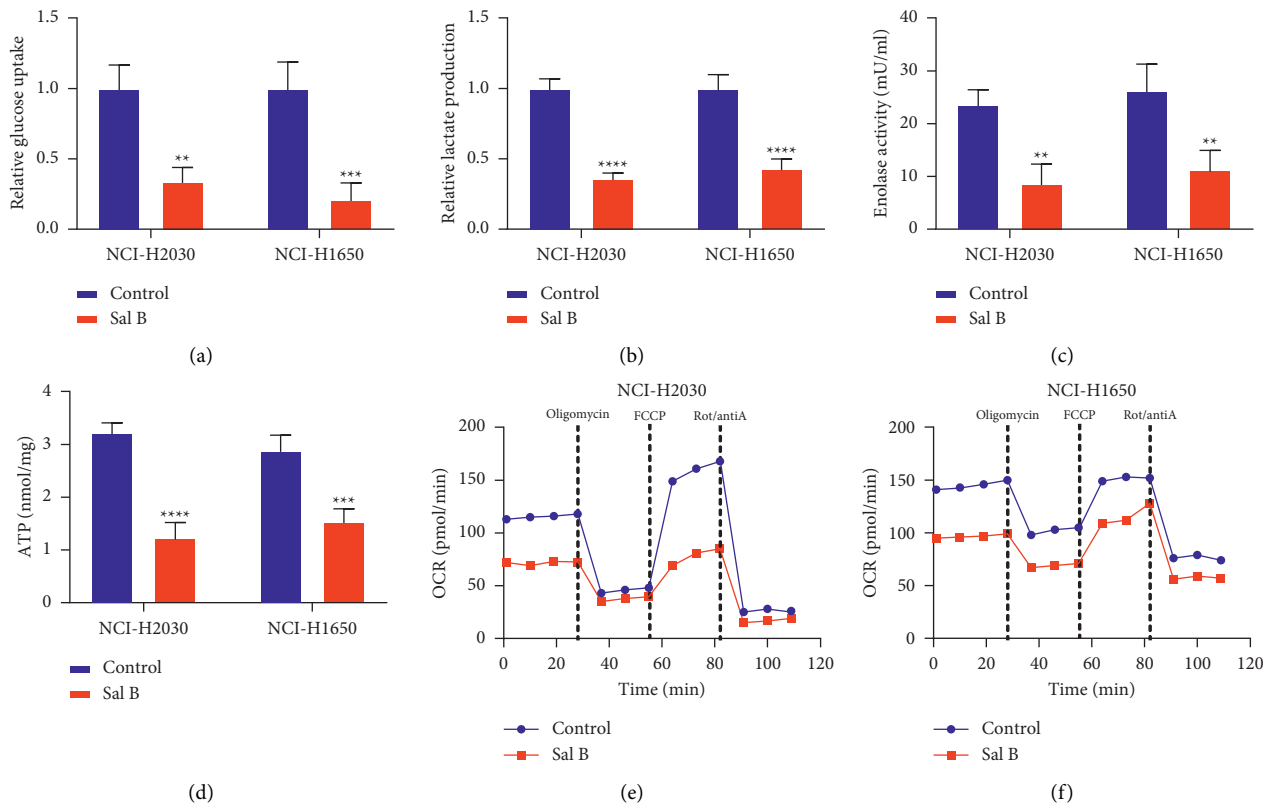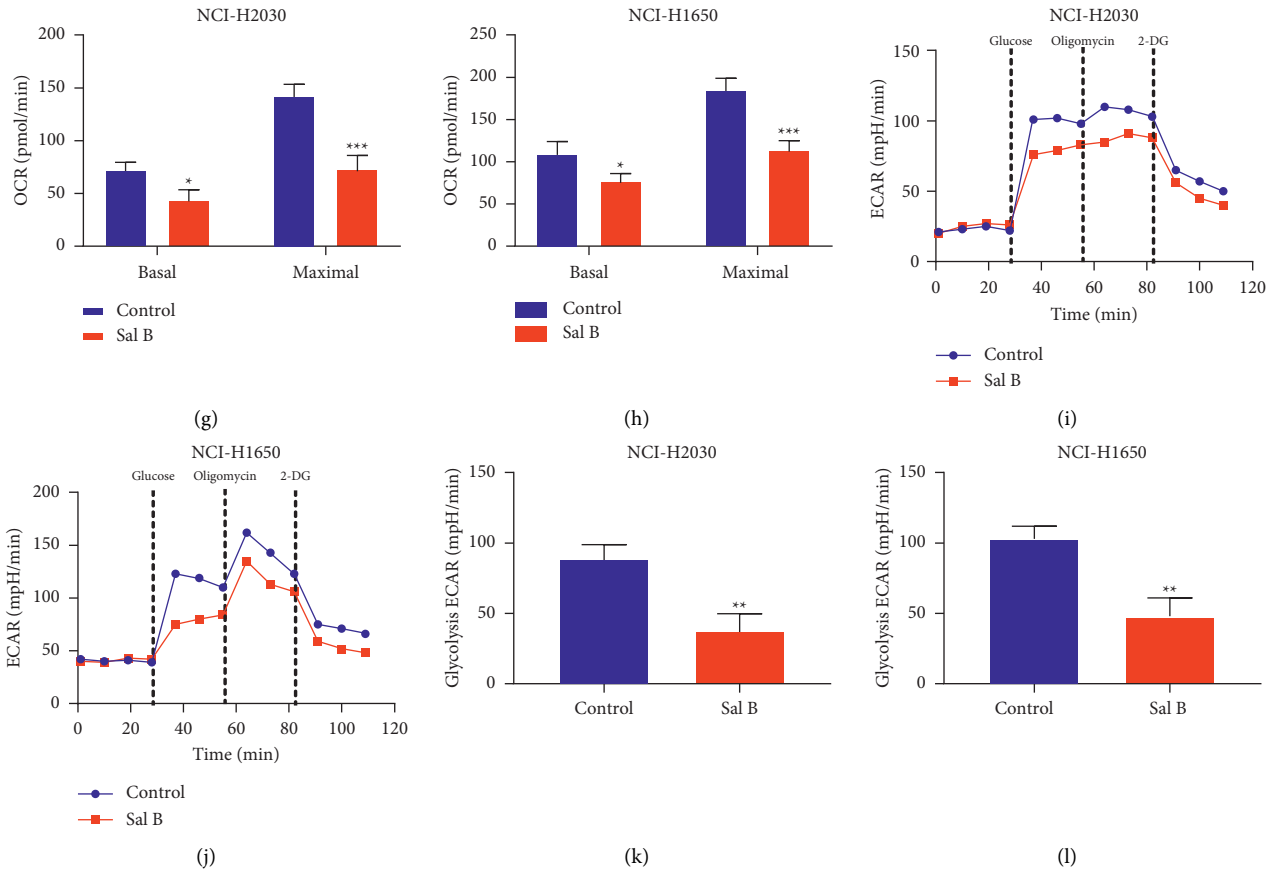
FIGURE 3: Sal B weakens metabolic reprogramming of NSCLC cells. (a–d) Glucose uptake, lactate production, enolase activity, as well as cellular ATP production of 200 μM Sal B-treated NCI-H2030 and NCI-H1650 cells. (e, f) Measurement of OCR of 200 μM Sal B-treated two NSCLC cells when exposure to oligomycin, FCCP, and Rot/antiA. (g, h) Quantification of basal and maximal OCR of 200 μM Sal B-treated two NSCLC cells. (i, j) Measurement of ECAR of 200 μM Sal B-treated two NSCLC cells after exposing to glucose, oligomycin, and 2-DG. (k, l) Quantification of glycolysis ECAR of above two NSCLC cells. $*P < 0.05$; $**P < 0.01$; $***P < 0.001$; $****P < 0.0001$.
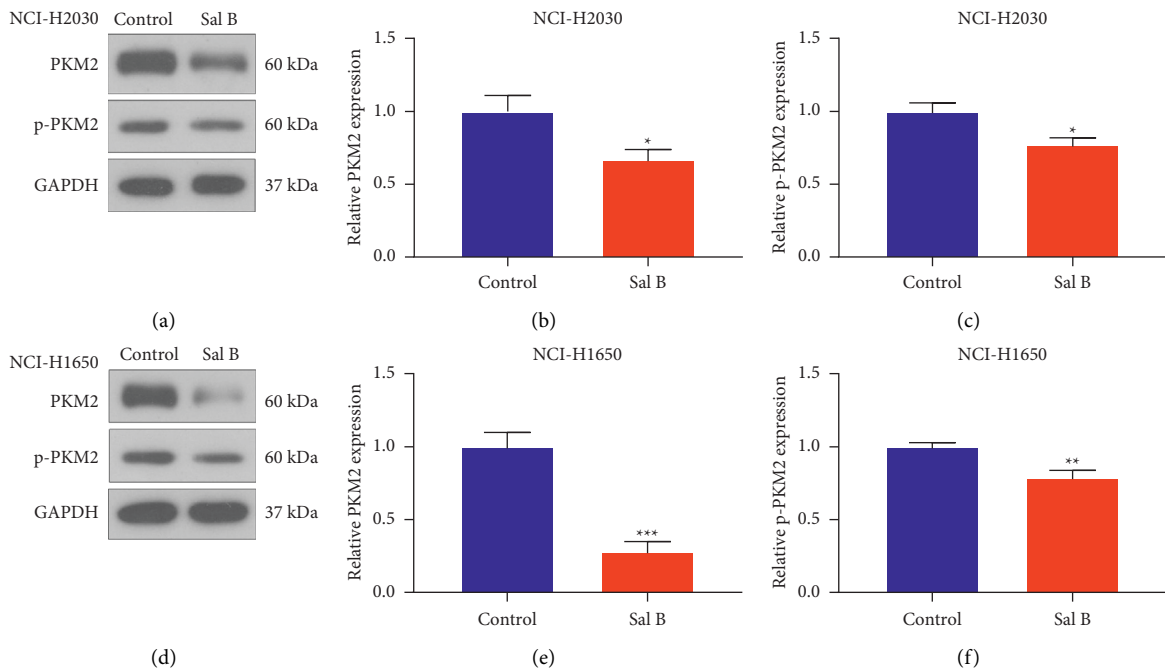

(a)

(b)

(c)

(d)

(e)

(f)

FIGURE 4: Continued.

NCI-H2030

Control   Sal B

DAPI

PKM2

Merge
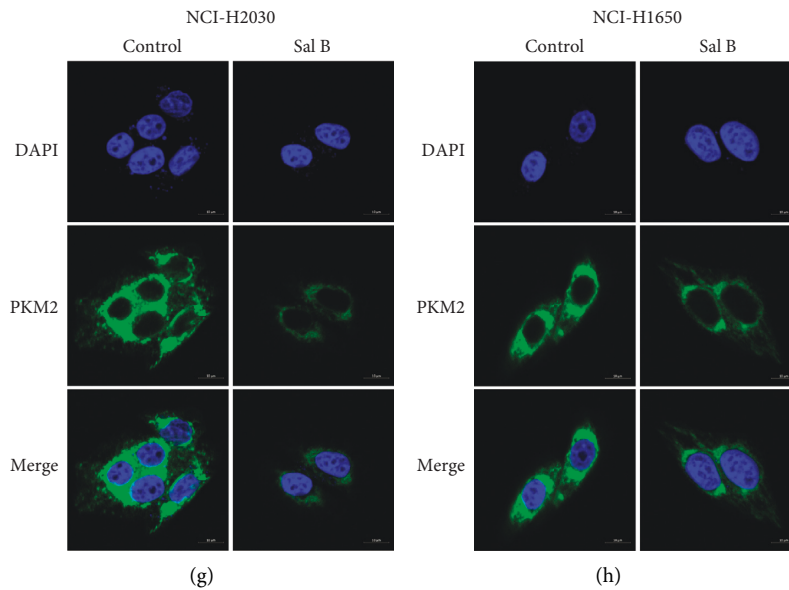
(g)

NCI-H1650

Control   Sal B

DAPI

PKM2

Merge

(h)

FIGURE 4: Sal B inhibits PKM2-mediated metabolic reprogramming of NSCLC cells. (a–c) Western blots for PKM2 as well as p-PKM2 expressions in 200 μM Sal B-treated NCI-H2030 cells. (d–f) Western blots for PKM2 as well as p-PKM2 expressions in 200 μM Sal B-exposed NCI-H1650 cells. (g, h) Immunofluorescence for investigating PKM2 expression in 200 μM Sal B-exposed NCI-H2030 and NCI-H1650 cells. Bar = 10 μM. $^{*}P < 0.05$; $^{**}P < 0.01$; $^{***}P < 0.001$.

and NCI-H2030 cells (Figures 5(a)–5(f)). Immunohisto-chemistry also confirmed the decreased expression of GLUT1 in 200 μM Sal B-treated NCI-H2030 as well as NCI-H2030 cells (Figures 5(g) and 5(h)).

3.6. Sal B Suppresses Migration and Invasion of NSCLC Cells via PKM2-Independent Metabolic Reprogramming. We conducted further analysis to demonstrate whether Sal B restrained NSCLC metastasis with PKM2-independent metabolic reprogramming. 10 μM TEPP-46 was utilized for selectively activating PKM2 expression. As shown in wound healing, TEPP-46 markedly weakened the inhibitory effects of Sal B on the migration capacity of NCI-H2030 and NCI-H1650 cells (Figures 6(a)–6(d)). Additionally, transwell results demonstrated that TEPP-46 enabled to reverse the inhibitory effects of Sal B on the invasion capacity of NCI-H2030 and NCI-H1650 cells (Figures 6(e)–6(g)). Altogether, Sal B may suppress NSCLC metastasis via PKM2-independent metabolic reprogramming.

3.7. Sal B Weakens EMT Process of NSCLC Cells through PKM2-Independent Metabolic Reprogramming. As expected, TEPP-46 was capable of enhancing PKM2 and GLUT1 expression in Sal B-exposed NCI-H2030 as well as NCI-H1650 cells (Figures 7(a)–7(j)), demonstrating that TEPP-46 markedly reversed the inhibitory effects of Sal B on metabolic reprogramming of NSCLC cells. Further analysis demonstrated that TEPP-46 administration enhanced β-catenin expression as well as decreased E-cadherin expression in Sal B-treated NCI-H2030 and NCI-H1650 cells (Figures 7(a)–7(j)). Thus, Sal B weakened EMT

activation of NSCLC cells with PKM2-independent metabolic reprogramming.

4. Discussion

NSCLC is a fatal malignancy with a hallmark of abnormal metabolism [22]. Sal B represents a dominating water-soluble component extracted from Salvia miltiorrhiza [23]. Our data demonstrated that Sal B was capable of weakening NSCLC metastasis with PKM2-independent metabolic reprogramming.

Metastasis represents an extremely complex multistage process [24]. Tumor cells are detached from the extracellular matrix and then colonize surrounding environment, demonstrating that benign nodules transform to aggressive malignancies [25–27]. Sal B-treated NCI-H2030 and NCI-H1650 cells displayed reduced migration and invasion capacities, indicating the inhibitory effect of Sal B on NSCLC metastasis. Previous research has demonstrated that Sal B may restrain the migration and invasion of hepatocellular carcinoma through RECK/STAT3 signaling [28]. For crossing the basement membrane along with the basal layer, tumor cells are functionally and morphologically altered through activating EMT that has the features of upregulation of β-cadherin and downregulation of E-cadherin [29]. Sal B administration enabled the decrease β-cadherin expression as well as the enhancement of E-cadherin expression of NCI-H2030 and NCI-H1650 cells, demonstrating the inactivation of EMT in NSCLC cells. Previous evidence has proposed that Sal B is capable of suppressing EMT to alleviate drug resistance via AKT/mTOR signaling in gastric cancer [30].

Tumor cells usually reprogram the metabolism to effectively support cell proliferation and survival [31]. Herein, Sal B treatment markedly reduced glucose uptake, lactate
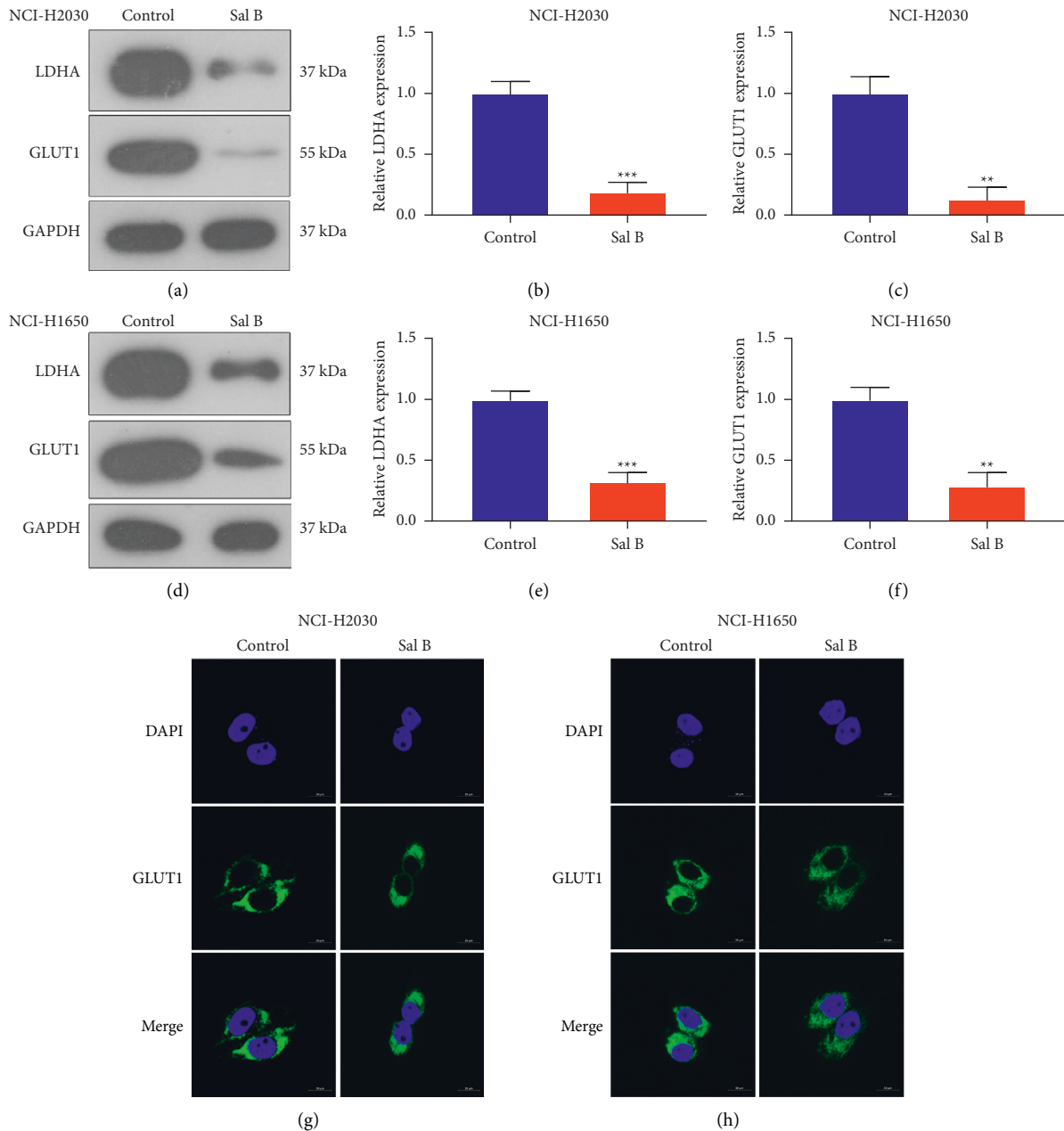
(a)

(b)

(c)

(d)

(e)

(f)

(g)

(h)

FIGURE 5: Sal B restrains metabolic reprogramming-relevant genes LDHA and GLUT1 in NSCLC cells. (a–f) Western blots for measuring LDHA and GLUT1 expressions in 200 μM Sal B-treated NCI-H2030 as well as NCI-H2030 cells. (g, h) Immunofluorescence for investigating the expression of LDHA and GLUT1 in 200 μM Sal B-exposed NCI-H2030 and NCI-H1650 cells. Bar = 10 μM. $^{**}P < 0.01$; $^{***}P < 0.001$.

production, enolase activity, cellular ATP production, OCR, and ECAR of NCI-H2030 and NCI-H1650 cells, demonstrating that Sal B weakened the metabolic reprogramming of NSCLC cells. Limited evidence has proposed the suppression effect of Sal B on metabolic reprogramming. For instance, Sal B may weaken glycolysis in oral squamous cell carcinoma through PI3K/AKT/HIF-1α signaling [15]. Additionally, Sal B reduces M1-polarized macrophages in myocardial ischemia/ reperfusion damage through weakening mTORC1-dependent glycolysis [32–34]. PKM2 is a crucial regulator of metabolic reprogramming, which may catalyze the synthesis of pyruvate from phosphoenolpyruvate and facilitate glycolysis, thereby

allowing tumor cells to thrive [35, 36]. Hypoxia-triggered exosomes transmit cisplatin resistance to sensitive NSCLC cells through delivery of PKM2 [22]. PKM2 facilitates HSP90-independent stability of IGF-1R precursor protein as well as enhances growth of cancer cells in a hypoxic environment [36]. eEF2 kinase-triggered inactivated STAT3 may inhibit the proliferative capacity of NSCLC cells through phosphorylation of PKM2 [37]. TEAD4 enables to enhance NSCLC progression with PKM2-mediated glycolysis [38]. Silencing PKM2 may retrain tumor growth as well as invasion in NSCLC [39]. Altogether, accumulated pieces of evidence have provided the basic data required for PKM2-targeted gene therapy. Sal B may
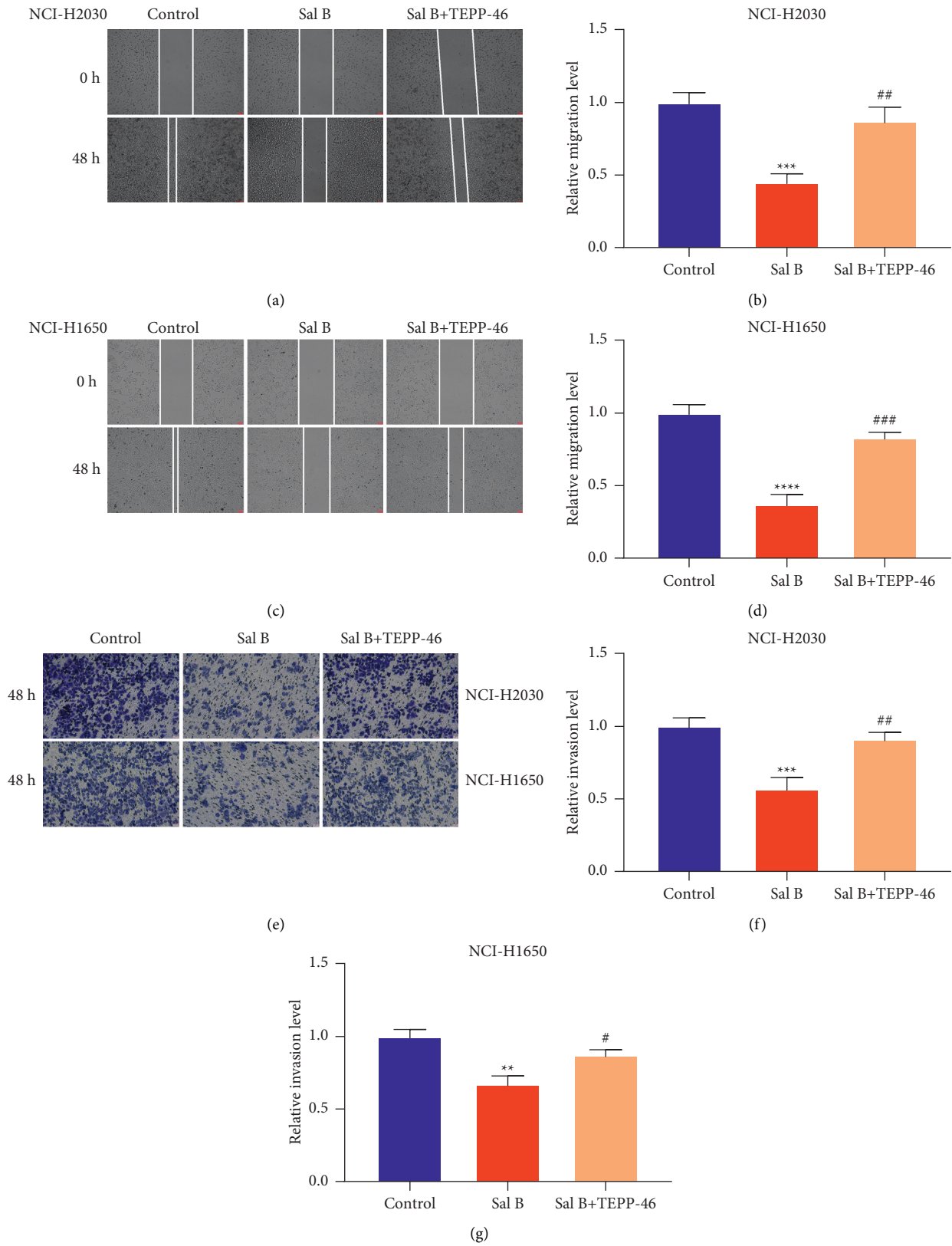
(a)

(b)

(c)

(d)

(e)

(f)

(g)

FIGURE 6: Sal B suppresses migration and invasion of NSCLC cells via PKM2-independent metabolic reprogramming. (a–d) Wound healing of the migration of NCI-H2030 and NCI-H1650 cells when exposure to 200 μM Sal B or 10 μM TEPP-46. Bar = 50 μM. (e–g) Transwell for evaluating the invasion of NCI-H2030 and NCI-H1650 cells following exposure to 200 μM Sal B or 10 μM TEPP-46. Bar = 50 μM. Compared with control group, $^{**}P < 0.01$; $^{***}P < 0.001$; $^{****}P < 0.0001$. Compared with Sal B group, $^{#}P < 0.05$; $^{##}P < 0.01$; $^{###}P < 0.001$.
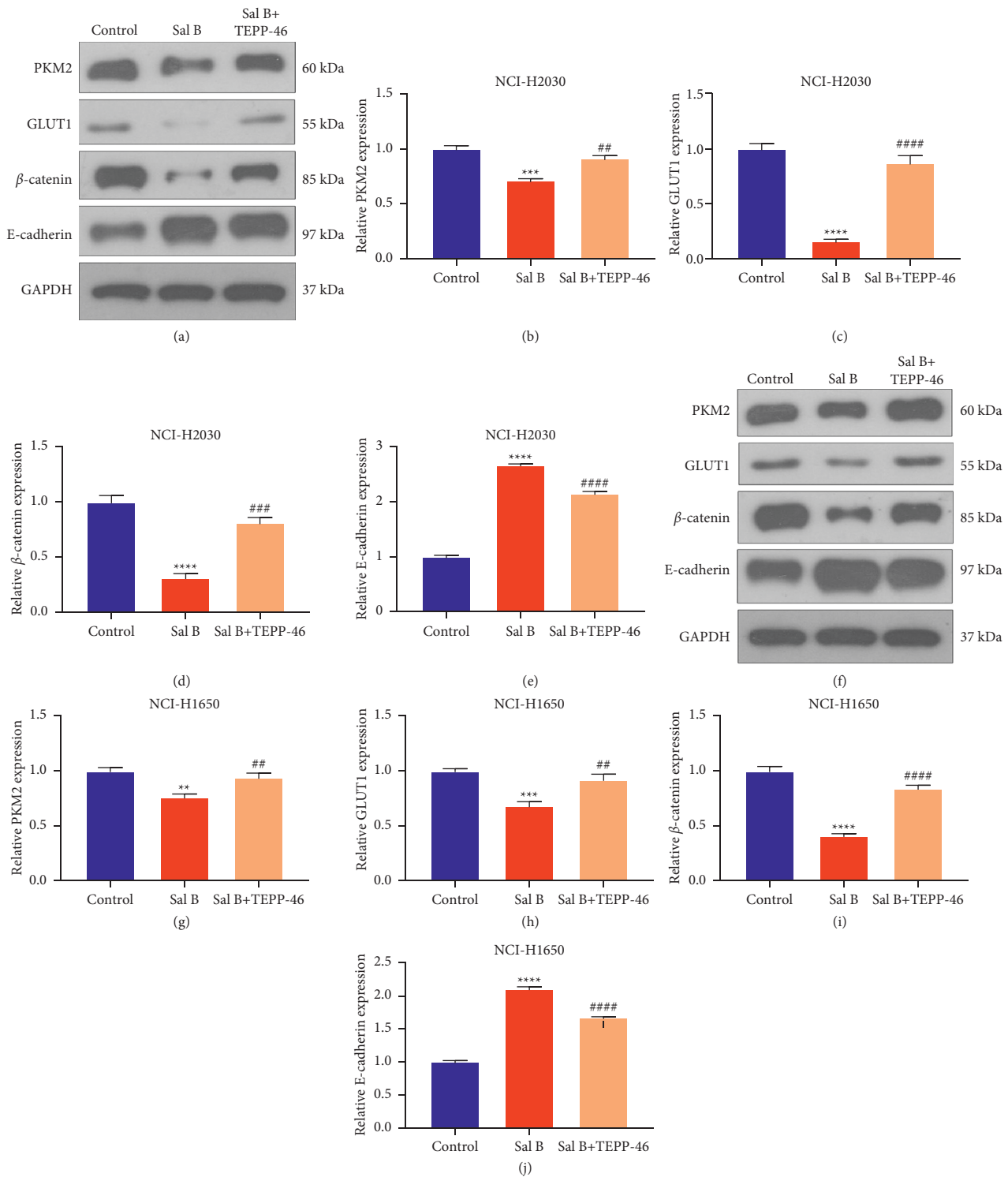
(a)

(b)

(c)

(d)

(e)

(f)

(g)

(h)

(i)

(j)

Figure 7: Sal B weakens EMT process of NSCLC cells through PKM2-independent metabolic reprogramming. (a–e) Western blotting for evaluating PKM2, GLUT1, β-catenin, and E-cadherin expressions in NCI-H2030 cells when exposure to $200\,\mu$M Sal B or $10\,\mu$M TEPP-46. (f–j) Western blotting of PKM2, GLUT1, β-catenin, and E-cadherin expressions in NCI-H1650 cells following exposure to $200\,\mu$M Sal B or $10\,\mu$M TEPP-46. Compared with control group, $^{**}P < 0.01$; $^{***}P < 0.001$; $^{****}P < 0.0001$. Compared with Sal B group, $^{\#\#}P < 0.01$; $^{\#\#\#}P < 0.001$; $^{\#\#\#\#}P < 0.0001$.

lower PKM2 expression and its phosphorylation in NCI-H2030 and NCI-H1650 cells.

LDHA and GLUT1 are crucial components of the glycolytic signaling [40]. LDHA [41] and GLUT1 [42] both display upregulation in NSCLC than normal tissues, which enable to independently predict undesirable clinical outcomes. LDHA activation may enhance the growth of NSCLC [43], and miR-449a weakens LDHA-independent glycolysis

to strengthen the sensitivity of NSCLC cells to ionizing radiotherapy [44]. NSCLC growth and radiotherapy resistance depend upon GLUT1-independent glucose uptake in tumor-associated neutrophils [45]. LDHA and GLUT1 expression was decreased by Sal B in NCI-H2030 and NCI-H1650 cells, demonstrating the inhibitory function of Sal B in glycolytic signaling of NSCLC cells. Metabolic reprogramming represents a hallmark of cancer metastases [46, 47], and tumor cells manipulate the metabolic profiles to meet the dynamic energy demands of the tumor microenvironment [48–50]. The data showed that Sal B enabled to weaken NSCLC metastasis with PKM2-independent metabolic reprogramming. In future studies, in vivo experiments are required for demonstrating the therapeutic efficacy of Sal B in NSCLC metastasis.

5. Conclusion

Altogether, this study provided evidence that Sal B was capable of weakening NSCLC metastasis via PKM2-independent metabolic reprogramming, shedding light on the promising therapeutic usage of Sal B in NSCLC therapy.

Abbreviations

NSCLC: Non-small-cell lung cancer
PKM2:   Pyruvate kinase M2
Sal-B: Salvianolic acid B
FBS: Fetal bovine serum
CCK-8:   Cell counting kit-8
p-PKM2: Phosphorylated PKM2
LDHA: Lactate dehydrogenase A
GLUT1:   Glucose transporter 1
OCR: Oxygen consumption rate
ECAR: Extracellular acidification rate
FCCP: Carbonyl-cyanide p-trifluoromethoxy phenylhydrazone
antiA: Antimycin A
Rot: Rotenone
2-DG: 2-Deoxyglucose
ANOVA: One-way analysis of variance.

Data Availability

The datasets analyzed during the current study are available from the corresponding author on reasonable request.

Conflicts of Interest

The authors declare no conflicts of interest.

References

[1] T. Singh, M. Fatehi Hassanabad, and A. Fatehi Hassanabad, "Non-small cell lung cancer: emerging molecular targeted and immunotherapeutic agents," *Biochimica et Biophysica Acta. Reviews on Cancer*, vol. 1876, no. 2, Article ID 188636, 2021.

[2] X. Zhu, L. Chen, L. Liu, and X. Niu, "EMT-mediated acquired EGFR-TKI resistance in NSCLC: mechanisms and strategies," *Frontiers in Oncology*, vol. 9, p. 1044, 2019.

[3] P. A. VanderLaan and S. Roy-Chowdhuri, "Current and future trends in non-small cell lung cancer biomarker testing: the American experience," *Cancer Cytopathology*, vol. 128, no. 9, pp. 629–636, 2020.

[4] R. Remark, C. Becker, J. E. Gomez et al., "The non-small cell lung cancer immune contexture. A major determinant of tumor characteristics and patient outcome," *American Journal of Respiratory and Critical Care Medicine*, vol. 191, no. 4, pp. 377–390, 2015.

[5] N. Kim, H. K. Kim, K. Lee et al., "Single-cell RNA sequencing demonstrates the molecular and cellular reprogramming of metastatic lung adenocarcinoma," *Nature Communications*, vol. 11, no. 1, p. 2285, 2020.

[6] S. P. L. Saw, B.-H. Ong, K. L. M. Chua, A. Takano, and D. S. W. Tan, "Revisiting neoadjuvant therapy in non-small-cell lung cancer," *Lancet Oncology*, vol. 22, no. 11, pp. e501–e516, 2021.

[7] E. Kozłowska, R. Suwiński, M. Giglok, A. Świerniak, and M. Kimmel, "Mathematical model predicts response to chemotherapy in advanced non-resectable non-small cell lung cancer patients treated with platinum-based doublet," *PLoS Computational Biology*, vol. 16, no. 10, Article ID e1008234, 2020.

[8] H. Wakabayashi, H. Arai, and A. Inui, "The regulatory approval of anamorelin for treatment of cachexia in patients with non-small cell lung cancer, gastric cancer, pancreatic cancer, and colorectal cancer in Japan: facts and numbers," *Journal of Cachexia, Sarcopenia and Muscle*, vol. 12, no. 1, pp. 14–16, 2021.

[9] M. Wang, R. S. Herbst, and C. Boshoff, "Toward personalized treatment approaches for non-small-cell lung cancer," *Nature Medicine*, vol. 27, no. 8, pp. 1345–1356, 2021.

[10] C. M. Dowling, H. Zhang, T. N. Chonghaile, and K.-K. Wong, "Shining a light on metabolic vulnerabilities in non-small cell lung cancer," *Biochimica et Biophysica Acta. Reviews on Cancer*, vol. 1875, no. 1, Article ID 188462, 2021.

[11] P.-H. Chen, L. Cai, K. Huffman et al., "Metabolic diversity in human non-small cell lung cancer cells," *Molecular Cell*, vol. 76, no. 5, pp. 838–851, 2019.

[12] H. Chang, Q. Xu, J. Li et al., "Lactate secreted by PKM2 upregulation promotes galectin-9-mediated immunosuppression via inhibiting NF-κB pathway in HNSCC," *Cell Death and Disease*, vol. 12, no. 8, p. 725, 2021.

[13] Q. Hua, B. Mi, F. Xu et al., "Hypoxia-induced lncRNA-AC020978 promotes proliferation and glycolytic metabolism of non-small cell lung cancer by regulating PKM2/HIF-1α axis," *Theranostics*, vol. 10, no. 11, pp. 4762–4778, 2020.

[14] C. Wang, S. Zhang, J. Liu et al., "Secreted pyruvate kinase M2 promotes lung cancer metastasis through activating the integrin Beta1/FAK signaling pathway," *Cell Reports*, vol. 30, no. 6, pp. 1780–1797, 2020.

[15] J. Wei, J. Wu, W. Xu et al., "Salvianolic acid B inhibits glycolysis in oral squamous cell carcinoma via targeting PI3K/AKT/HIF-1α signaling pathway," *Cell Death and Disease*, vol. 9, no. 6, p. 599, 2018.

[16] G. H. Li, Y. R. Li, P. Jiao et al., "Therapeutic potential of *Salviae miltiorrhizae* radix et rhizoma against human diseases based on activation of Nrf2-mediated antioxidant defense system: bioactive constituents and mechanism of action," *Oxidative Medicine and Cellular Longevity*, vol. 2018, Article ID 7309073, 2018.

[17] M. A. Katary, R. Abdelsayed, A. Alhashim, M. Abdelhasib, and A. A. Elmarakby, "Salvianolic acid B slows the progression of breast cancer cell growth via enhancement of

apoptosis and reduction of oxidative stress, inflammation, and angiogenesis," *International Journal of Molecular Sciences*, vol. 20, 2019.

[18] W. Chen, N. Wang, R.-C. Li et al., "Salvianolic acid B renders glioma cells more sensitive to radiation via Fis-1-mediated mitochondrial dysfunction," *Biomedicine and Pharmacotherapy*, vol. 107, pp. 1230–1236, 2018.

[19] Y. Hao, T. Xie, A. Korotcov et al., "Salvianolic acid B inhibits growth of head and neck squamous cell carcinoma in vitro and in vivo via cyclo oxygenase-2 and apoptotic pathways," *International Journal of Cancer*, vol. 124, no. 9, pp. 2200–2209, 2009.

[20] Y. Adachi, K. Ito, Y. Hayashi et al., "Epithelial-to-mesenchymal transition is a cause of both intrinsic and acquired resistance to KRAS G12C inhibitor in KRAS G12C-mutant non-small cell lung cancer," *Clinical Cancer Research*, vol. 26, no. 22, pp. 5962–5973, 2020.

[21] M. K. Nayak, M. Ghatge, G. D. Flora et al., "The metabolic enzyme pyruvate kinase M2 regulates platelet function and arterial thrombosis," *Blood*, vol. 137, no. 12, pp. 1658–1668, 2021.

[22] D. Wang, C. Zhao, F. Xu et al., "Cisplatin-resistant NSCLC cells induced by hypoxia transmit resistance to sensitive cells through exosomal PKM2," *Theranostics*, vol. 11, no. 6, pp. 2860–2875, 2021.

[23] J. Qiao, A. Liu, J. Liu, D. Guan, and T. Chen, "Salvianolic acid B (Sal B) alleviates the decreased activity induced by prednisolone acetate on osteoblasts by up-regulation of bone formation and differentiation genes," *Food and Function*, vol. 10, no. 9, pp. 6184–6192, 2019.

[24] Y. Sun, X. Niu, G. Wang, X. Qiao, L. Chen, and M. Zhong, "A novel lncRNA ENST00000512916 facilitates cell proliferation, migration and cell cycle progression in ameloblastoma," *OncoTargets and Therapy*, vol. 3, pp. 1519–1531, 2020.

[25] G. Pan, Y. Liu, L. Shang, F. Zhou, and S. Yang, "EMT-associated microRNAs and their roles in cancer stemness and drug resistance," *Cancer Communications*, vol. 41, no. 3, pp. 199–217, 2021.

[26] X. Wang, G. Cheng, Y. Miao et al., "Piezo type mechanosensitive ion channel component 1 facilitates gastric cancer omentum metastasis," *Journal of Cellular and Molecular Medicine*, vol. 25, no. 4, pp. 2238–2253, 2021.

[27] R. Ren, Y. Du, X. Niu, and R. Zang, "ZFPM2-AS1 transcriptionally mediated by STAT1 regulates thyroid cancer cell growth, migration and invasion via miR-515-5p/TUSC3," *Journal of Cancer*, vol. 12, no. 11, pp. 3393–3406, 2021.

[28] M. Teng, C. Hu, B. Yang et al., "Salvianolic acid B targets mortalin and inhibits the migration and invasion of hepatocellular carcinoma via the RECK/STAT3 pathway," *Cancer Cell International*, vol. 21, no. 1, p. 654, 2021.

[29] X. Qiao, X. Niu, J. Shi et al., "Wnt5a regulates ameloblastoma cell migration by modulating mitochondrial and cytoskeletal dynamics," *Journal of Cancer*, vol. 11, no. 18, pp. 5490–5502, 2020.

[30] J. Wang, Y. Ma, M. Guo, H. Yang, and X. Guan, "Salvianolic acid B suppresses EMT and apoptosis to lessen drug resistance through AKT/mTOR in gastric cancer cells," *Cytotechnology*, vol. 73, no. 1, pp. 49–61, 2021.

[31] X. Wang, R. Liu, W. Zhu et al., "UDP-glucose accelerates SNAI1 mRNA decay and impairs lung cancer metastasis," *Nature*, vol. 571, no. 7763, pp. 127–131, 2019.

[32] X. Kong, M. Fu, X. Niu, and H. Jiang, "Comprehensive analysis of the expression, relationship to immune infiltration

and prognosis of TIM-1 in cancer," *Frontiers in Oncology*, vol. 10, p. 1086, 2020.

[33] X. Liu, X. Niu, and Z. Qiu, "A five-gene signature based on stromal/immune scores in the tumor microenvironment and its clinical implications for liver cancer," *DNA and Cell Biology*, vol. 39, no. 9, pp. 1621–1638, 2020.

[34] M. Zhao, F. Li, Y. Jian et al., "Salvianolic acid B regulates macrophage polarization in ischemic/reperfused hearts by inhibiting mTORC1-induced glycolysis," *European Journal of Pharmacology*, vol. 871, Article ID 172916, 2020.

[35] D. Anastasiou, G. Poulogiannis, J. M. Asara et al., "Inhibition of pyruvate kinase M2 by reactive oxygen species contributes to cellular antioxidant responses," *Science*, vol. 334, no. 6060, pp. 1278–1283, 2011.

[36] H. Koo, S. Byun, J. Seo et al., "PKM2 regulates HSP90-mediated stability of the IGF-1R precursor protein and promotes cancer cell survival during hypoxia," *Cancers*, vol. 13, no. 15, 2021.

[37] M. Xiao, J. Xie, Y. Wu et al., "The eEF2 kinase-induced STAT3 inactivation inhibits lung cancer cell proliferation by phosphorylation of PKM2," *Cell Communication and Signaling*, vol. 18, no. 1, p. 25, 2020.

[38] Y. Hu, H. Mu, and Z. Deng, "The transcription factor TEAD4 enhances lung adenocarcinoma progression through enhancing PKM2 mediated glycolysis," *Cell Biology International*, vol. 45, no. 10, pp. 2063–2073, 2021.

[39] H. Sun, A. Zhu, L. Zhang, J. Zhang, Z. Zhong, and F. Wang, "Knockdown of PKM2 suppresses tumor growth and invasion in lung adenocarcinoma," *International Journal of Molecular Sciences*, vol. 16, no. 10, pp. 24574–24587, 2015.

[40] N. Huo, R. Cong, Z.-J. Sun et al., "STAT3/LINC00671 axis regulates papillary thyroid tumor growth and metastasis via LDHA-mediated glycolysis," *Cell Death and Disease*, vol. 12, no. 9, p. 799, 2021.

[41] C. Yu, L. Hou, H. Cui et al., "LDHA upregulation independently predicts poor survival in lung adenocarcinoma, but not in lung squamous cell carcinoma," *Future Oncology*, vol. 14, no. 24, pp. 2483–2492, 2018.

[42] B. Zhang, Z. Xie, and B. Li, "The clinicopathologic impacts and prognostic significance of GLUT1 expression in patients with lung cancer: a meta-analysis," *Gene*, vol. 689, pp. 76–83, 2019.

[43] X. Wang, X. Xie, Y. Zhang et al., "Hippocalcin-like 1 is a key regulator of LDHA activation that promotes the growth of non-small cell lung carcinoma," *Cellular Oncology*, vol. 45, 2022.

[44] L. Li, H. Liu, L. Du et al., "miR-449a suppresses LDHA-mediated glycolysis to enhance the sensitivity of non-small cell lung cancer cells to ionizing radiation," *Oncology Research Featuring Preclinical and Clinical Cancer Therapeutics*, vol. 26, no. 4, pp. 547–556, 2018.

[45] P.-B. Ancey, C. Contat, G. Boivin et al., "GLUT1 expression in tumor-associated neutrophils promotes lung cancer growth and resistance to radiotherapy," *Cancer Research*, vol. 81, no. 9, pp. 2345–2357, 2021.

[46] M. Peng, D. Yang, Y. Hou et al., "Intracellular citrate accumulation by oxidized ATM-mediated metabolism reprogramming via PFKP and CS enhances hypoxic breast cancer cell invasion and metastasis," *Cell Death and Disease*, vol. 10, no. 3, p. 228, 2019.

[47] R. Liu, Y. Li, L. Tian et al., "Gankyrin drives metabolic reprogramming to promote tumorigenesis, metastasis and drug resistance through activating β-catenin/c-Myc signaling

in human hepatocellular carcinoma," *Cancer Letters*, vol. 443, pp. 34–46, 2019.

[48] L. Chen, G. Wang, X. Qiao et al., "Downregulated miR-524-5p participates in the tumor microenvironment of ameloblastoma by targeting the interleukin-33 (IL-33)/Suppression of tumorigenicity 2 (ST2) Axis," *Medical Science Monitor: International Medical Journal of Experimental and Clinical Research*, vol. 26, Article ID e921863, 2020.

[49] X. Niu, L. Chen, Y. Li, Z. Hu, and F. He, "Ferroptosis, necroptosis, and pyroptosis in the tumor microenvironment: perspectives for immunotherapy of SCLC," *Seminars in Cancer Biology*, vol. 12, p. S1044, In press, 2022.

[50] J. Zhao, S. Zhong, X. Niu, J. Jiang, R. Zhang, and Q. Li, "The MHC class I-LILRB1 signalling axis as a promising target in cancer therapy," *Scandinavian Journal of Immunology*, vol. 90, Article ID e12804, 2019.